Determining fracture energy parameters of concrete from the modified compact tension test

A. Fernández-Canteli, L. Castañón, B. Nieto, M. Lozano
University of Oviedo, Gijón, Spain
afc@uniovi.es, labres@uniovi.es

T. Holušová, S. Seitl
Institute of Physics of Materials, Academy of Science of the Czech Republic, Brno, Czech Republic and
Brno University of Technology, Faculty of Civil Engineering, Institute of Structural Mechanics, Brno, Czech Republic
holusova.t@fce.vutbr.cz, seitl@ipm.cz

ABSTRACT. The modified compact tension (MCT) test, though not yet recognized as a valid test for determining fracture energy of concrete, is believed to represent a plausible and suitable alternative versus other well established procedures, such as the wedge-splitting test (WST) and the three point (3PB) or four point bending (4PB) tests, due to its simplicity and low cost. The aim of the paper is twofold: Firstly, to demonstrate the necessary correspondence between the experimental MCT test setup and finite element simulations and secondly, to initiate the way of establishing the desirable conversion between the fracture energy parameter values resulting from the MCT test and the standard conventional procedures. MCT tests are carried out and compared with the numerical results from 2-D and 3-D finite element calculations using the commercial codes ABAQUS and ATENA, the latter being specifically developed for applications on concrete structures and elements. In this way, the usability of the modified compact tension test for practical purposes is confirmed.

KEYWORDS. Concrete fracture energy; Modified compact tension test; Concrete; Numerical simulation.

INTRODUCTION AND MOTIVATION

One of the relevant parameters that characterize concrete fracture is its fracture energy. The most extended procedure for it to be obtained is the three point bending test [1 - 3], whose guidelines are collected in RILEM draft recommendation (50-FMC) [4, 5]. The wedge-splitting test [6, 7] represents some advantages compared to the three point bending test and it is also often used [8].

From any of those tests, the Load-displacement or Load-COD (crack open displacement) curve is obtained (Fig. 1) [9, 10], the area under which represents the work of fracture (W_f), from which the fracture energy (G_f) is defined as:

$$G_f = W_f / A_{lig} \tag{1}$$

where A_{lig} is a ligament area.

That previous kind of tests are carried out in testing machines implying specific devices and auxiliary tooling; moreover, the manufacture of such specimens is not simple; the test execution is far from being trivial and, finally, a relatively large

amount of material (especially for 3PB and 4PB) is needed. Searching for an alternative and simpler way of testing, the idea of using a compact tension (CT) specimen has emerged.

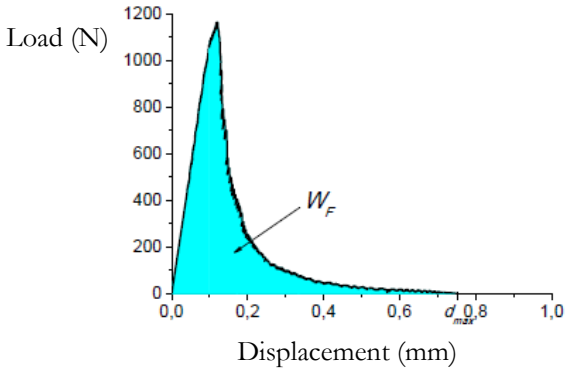

Figure 1: Load-displacement curve of concrete specimens

In metallic materials, testing CT specimens represents a usual procedure to determine fracture parameters. Thus, ASTM Standard E-399 [11, 12] specifies the geometry and general configuration of this kind of tests in metallic materials. The idea of its application to testing concrete on fracture is not new: previous researchers, like Wagoner et al. [13], attempt to perform this kind of tests in concrete according to the above mentioned standard though they ran into troubles obtaining premature failures in 50% of the tests at the pulling load holes thus evidencing the disability of the new procedure.
With the purpose of avoiding such a high percentage of invalid tests, a different CT test methodology, denoted modified compact tension test (MCT), is developed by the authors getting practically nil quote of premature failures. Basically, the new procedure consists in applying the pulling force by means of reinforced bars built in the specimen, which are clamped in the machine during testing [7, 14]. In this way, the need of providing holes in the specimen, as in the metallic materials, dismissed.

MODIFIED COMPACT TENSION TEST: CONFIGURATION

The modified compact tension test (MCT) solution was initially developed for slide shaped specimens cut off from cylindrical specimens used in standard compression tests, which can be obtained as a drill core from real constructions for evaluating age and conditions of the material. The holes are drilled into the specimens in perpendicular direction to the milled notch into which the pulling bars are allocated and glued. Nevertheless, in the meantime more advanced, practical and simple solutions, the denoted "ad-hoc" specimens, have been developed that facilitate its preparation in the laboratory. In the two above mentioned MCT solutions, i.e. "drill-out" and "ad-hoc" specimens, the geometry is apparently the same consisting in notched cylinders of a suitable thickness b furnished with the pulling bars, see Fig. 2, but they result from two different manufacturing procedures. The characteristic dimensions of the two specimens tested in this work are summarized in Tab. 1, where:
Π_{cs}: specimen diameter [mm],
Π_{sb}: pulling bar diameter [mm],
W: specimen width, i.e., distance from the load axis to the back side of the specimen [mm]
a: notch length measured from load axis [mm],
b: specimen thickness [mm],
e: notch width [mm],
A_{lig}: ligament area [mm^2], and
α: relative notch length [-].
With these values, the ligament area, defined as the area of specimen that has to be fractured, is calculated, as the product of the length of the ligament times the thickness of the specimen. On its turn, the relative notch length α, defined as the dimensionless parameter in Eq. (2) like in the original compact tension tests [15], is considered a reference parameter to be studied in the modified compact tension tests of concrete.

$$\alpha = a/W \tag{2}$$

with the same meaning of the parameters α , a and W as above.

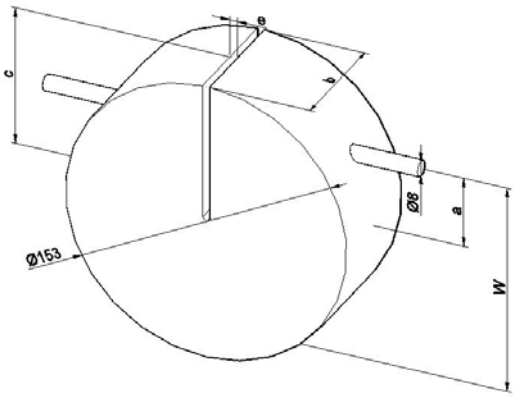

Figure 2: Characteristic specimen's dimensions in [mm].

	Π_{cs} [mm]	Π_{sb} [mm]	W [mm]	a [mm]	b [mm]	e [mm]	A_{lig} [mm^2]	α [-]
Specimen 1	153	8	116.4	40.2	63.5	4	4838.70	0.3454
Specimen 2	153	8	114.3	32.9	68.6	4	5584.04	0.2878

Table 1: Measured dimensions of the two specimens tested.

EXPERIMENTAL PROCEDURE

The fabrication of the specimens is as follows: firstly, concrete is prepared as a mixture of the components. Then, the concrete is poured into the mold, in this case a PVC pipe of internal diameter Π_d = 153 mm, i.e. the required for the specimen. The curing process lasted for 21 days after which the bars are allocated into the drill holes and glued to the specimen using a strong epoxy adhesive. Lastly, the notch is mechanized. This procedure can be also applied for fracture characterization of concrete when drilling cores are extracted from real structures.

All tests were performed with a servohydraulic test machine MTS Bionix 25 kN of load capacity, see Fig. 3. One of the bars is anchored to the lower clamps, which stay fixed. The other bar is anchored to the upper clamps, which move vertically up and transmit the load to the specimen. Thus, as the displacement of the upper clamp increases, a crack is generated starting in the tip of the notch, until the complete rupture of the specimen. Tests are performed by displacement control of the machine with a rate of 0.5 mm/min.

NUMERICAL SIMULATION

Numerical simulations are performed using two different codes based on the finite element method. The first one is the ATENA software [16, 17] developed for specific applications in concrete structures. The second one is the ABAQUS software [18]. The results from the compression test provide an average value of 32 MPa for the cylindrical compressive strength, which corresponds to a cubic compressive strength of 37 MPa. According to table 7 from European standard EN 206-1 (page 20), the concrete mixture was classified as C 30/37. A cubic compressive strength of 37 MPa was used as input value for the material model of concrete (SBETA) and after that the values of tensile strength and Young's modulus, etc. are calculated from empirical equations implemented in the ATENA software.

The characteristic input parameters of steel and concrete used in both cases of numerical simulations in ATENA and ABAQUS are listed in Tab. 2, where:

E: Young's modulus [MPa],
v: Poisson coefficient [-],
f_c: compressive strength of the concrete [MPa] and
f_t: tensile strength of the concrete [MPa].

Figure 3: Specimen set up into the servohydraulic MTS Bionix 25 kN machine.

	E [MPa]	*v* [-]	f_c [MPa]	f_t [MPa]
Steel	210000	0.3	-	-
Concrete	33010	0.2	31.45	2.665

Table 2: Mechanical input parameters for the material used in the ATENA and ABAQUS calculations.

In order to propitiate the factual non-symmetry behavior of the crack initiation at the notch and further propagation in the real specimen due to the non-uniformity of the aggregate, symmetry is disregarded so that the whole specimen is considered in the computations.

2D-Model 1 using ATENA code

An adaptation from the model of Holušová et al. [19] is performed for the new dimensions adopted as presented in Tab. 1, using the same commercial software ATENA 2D. The material is identified in ATENA as the model for concrete 3D Non Linear Cementitious 2 working under plain stress or plain strain conditions and SBETA that works only under plain strain condition, see [20,21]. Steel bars are there modeled as ideal lines, which simulate the pulling load axis of the testing machine. The mesh and boundary conditions are shown in Fig. 4. The size of elements is, typically, 2 mm with a refinement up to 1 mm around the starting notch.

2D-Model 2 using ABAQUS code with rigid bars

This model, created in ABAQUS, is based on the same premises as model 1, i.e. assuming the bars maintain a fixed pulling axis orientation during the test. This implies impeding any deviation or relative transversal displacement of the bars that unavoidably occurs during the real test as a consequence of the necessary compatibility between displacements of

both concrete specimen and pulling bars during the notch opening process thus provoking reactions and bending of the pulling bars. In this case, the bar is assumed to be perfectly rigid, so that the prescribed displacement in the pulling axis direction suffices to define the loading process. The material is modeled according to the so called "concrete damaged plasticity" model [22]. The mesh, load and boundary conditions are shown in Fig. 5. In this case, the size of the mesh is 5 mm, with a refinement in the ligament length up to 1 mm.

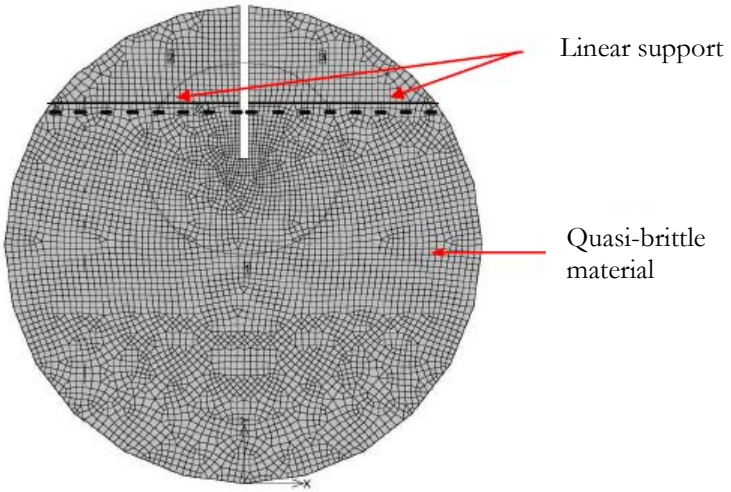

Figure 4: Mesh and boundary conditions used for model 1.

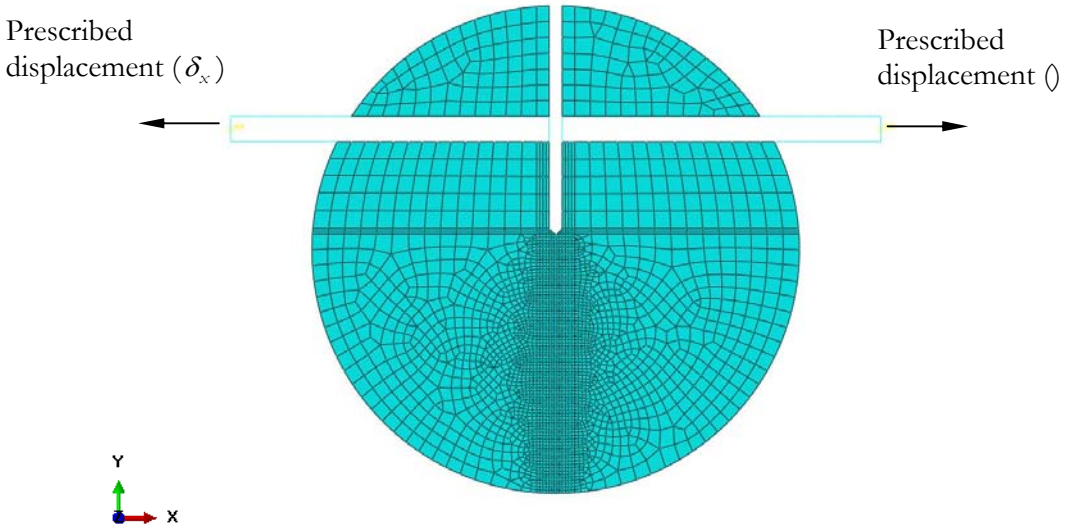

Figure 5: Mesh and boundary conditions for model 2.

3D-Model 3 using ABAQUS with free elastic lineal bars

This model, see Fig. 6, once more developed in ABAQUS code, represents loads and boundary conditions in a closer manner to the real modified compact tension test than the former two handled. A displacement in the longitudinal X-direction is prescribed at the end of the bars thus restricting the movement (displacement or rotation) in any other direction.

Modeling as 3D geometry implies considering a larger amount of elements. Due to non-symmetry reasons related to crack forming, as already exposed, no consideration of double symmetry, i.e. of a specimen quarter, is considered that would allow a significant reduction of the computational time. Exemplary, the element size is taken as 5 mm with a refinement up to 1 mm size in the ligament area and up to 3 mm in the perimeter of the hole where the bars are inserted.

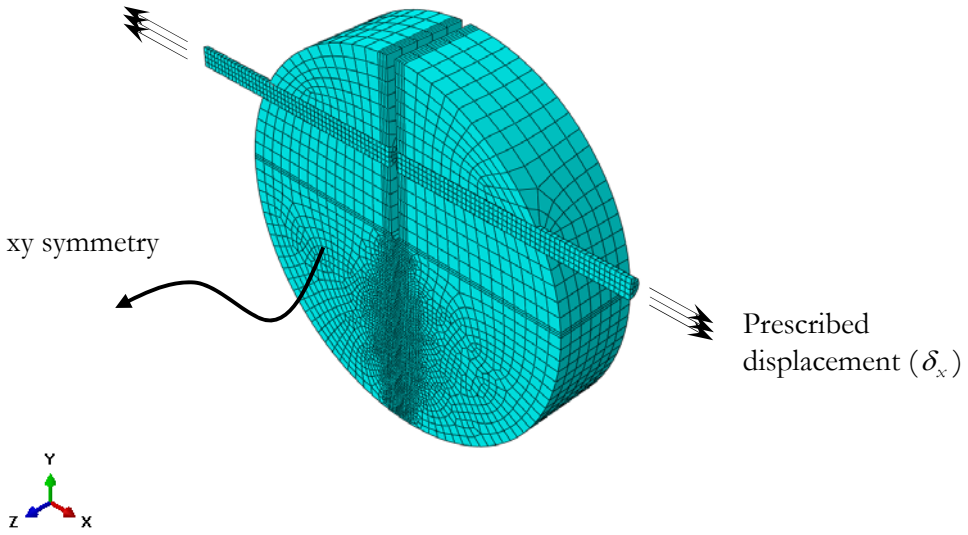

Figure 6: Mesh and boundary conditions for model 3.

3D-Model 4 using ABAQUS intermediate

In this model, the transversal displacement is prescribed only at the bar ends, identified with the machine clamps, but the transversal displacement of the notch mouth, u_y, is impeded. The model can be understood as a mixture between model 2 and model 3, see Fig. 7.

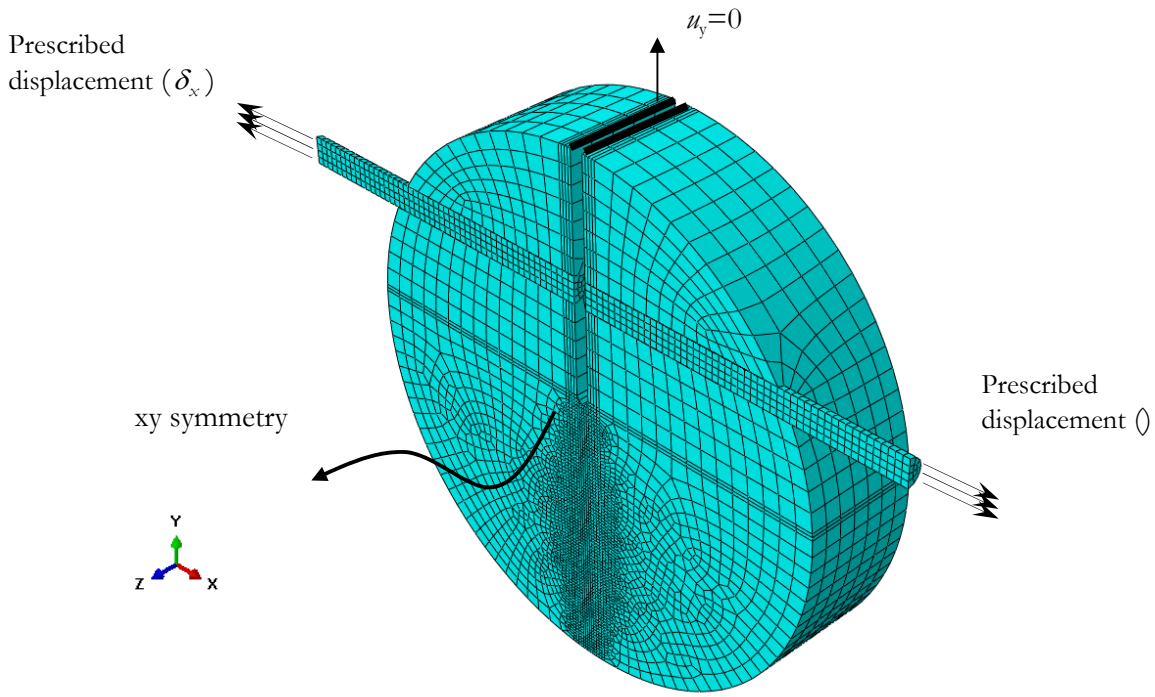

Figure 7: Mesh and boundary conditions for model 4.

RESULTS AND DISCUSSION

The Load-COD curves for every model are generated. The following graphs, see Figs. 8-9, show the numerical results obtained for the different numerical models and those from the experimental test for comparison.

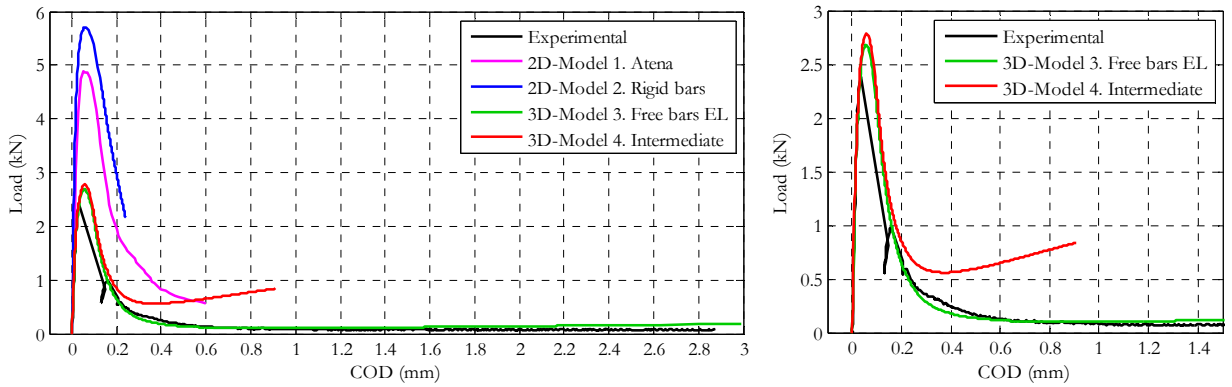

Figure 8: Load-COD curves for specimen 1: a) all modes including 2D model, and b) zoom detailing only 3D models and experimental results.

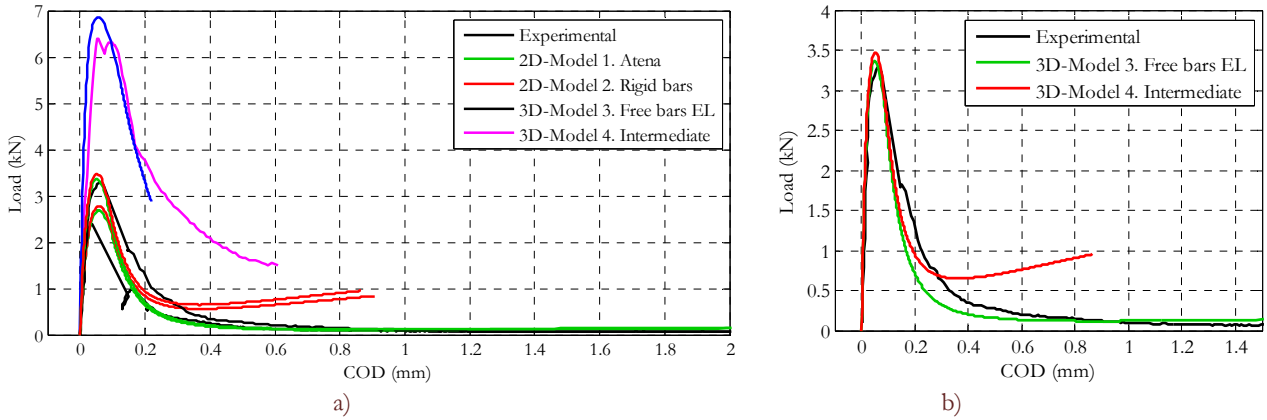

Figure 9: Load-COD curves for specimen 2: a) all modes including 2D model, and b) zoom detailing only 3D models and experimental results.

The theoretical difference between the cohesive model adopted in the ATENA code [16] and the smeared crack model used in ABAQUS [18] has not noticeable influence on the numerical results obtained.

- *Opening mechanisms*

There are two different forms in the evolution of the Load-COD curves obtained from models 1, 2, 3 and 4. These differences are related to the boundary conditions applied in the bars. Curves with higher maximum load emanate from models in which the transversal displacement is impeded along the total length of the bar. Otherwise, models with lower maximum load are only restricted at the ends of the bar. In consequence, models behavior is influenced by the enforced perpendicularity of the bars to the notch plane. As a result, two different notch opening mechanisms, parallel and angular ones, appear, see Fig. 10.

- *Influence of the transversal displacement in the fracture energy*

The first analysis of the model of MCT proposed by Holušová et al. [19], points out that the determinant factor explaining differences among the load-displacement curves is the restriction of the transversal Y-displacement of the model. That's why model 4 has been developed, changing from 2D to 3D and from a restriction in the length of the bars to a restriction in the notch mouth.

The results for this model, however, approaches the load-displacement curves of models 3 and 4 (see Figs. 8 and 9), especially in the initial ascending part of the curve. The maximum load is about the same, and the same applies for the initial region of the softening curve. Then, a new rise in the load happens, due to the difficulty of continuing crack opening.

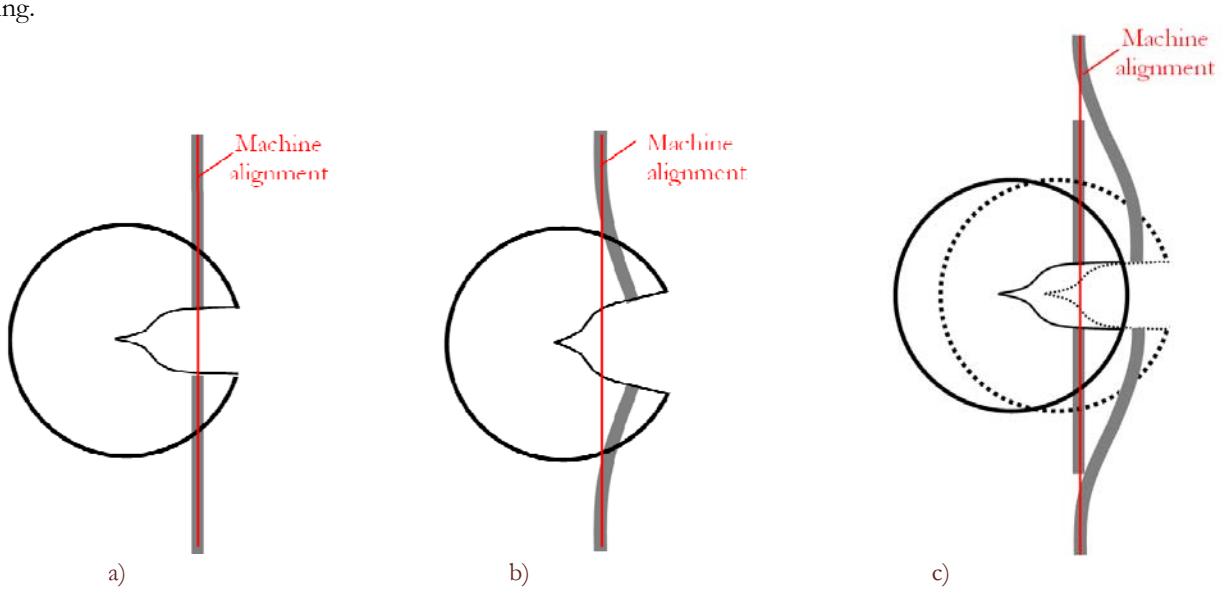

Figure 10: Schematic representation of the opening mechanism of the notch: a) parallel opening, b) angular opening and c) transversal displacement of the specimen during testing by parallel opening.

Models 1 and 2 correspond to a parallel opening, whilst models 3 and 4 generate an angular opening.

- *Correction of the Load-Displacement Curves*

Some problems appear in describing the softening part of the Load-COD curves in both experimental and simulation results. In most cases, the last part of the softening curve has an asymptotic behavior tending to a certain value of the load different from zero, instead of approaching gradually to null load, as it would be expected in a real case. Accordingly, a correction in the ordinate is introduced using the following equations, see Fig. 11:

$$y'(x) = x \tan\theta \tag{3}$$

$$y_{corrected}(x) = y(x) - y'(x) \tag{4}$$

where: θ = Angle between abscissa axis and the slope line *y'*. Line *y'* is formed by connecting the origin of the θ coordinate system with a far point, or eventually, the last point of the curve *y*.
tan θ = Slope of the line *y'*.

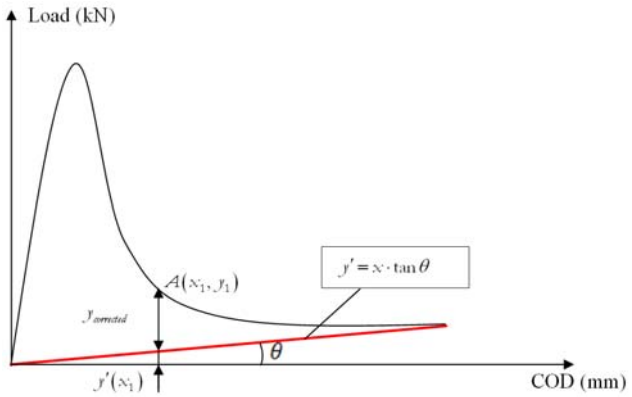

Figure 11: Scheme for the correction of the *y* axis.

Figures 12-13 show a) the experimental and b) the numerical load-COD curves for model 3 before and after introducing the correction, respectively, for specimen 1 and specimen 2, while Fig. 14 presents a direct comparison for the experimental and numerical energy curves for specimens 1 and 2 once corrected.

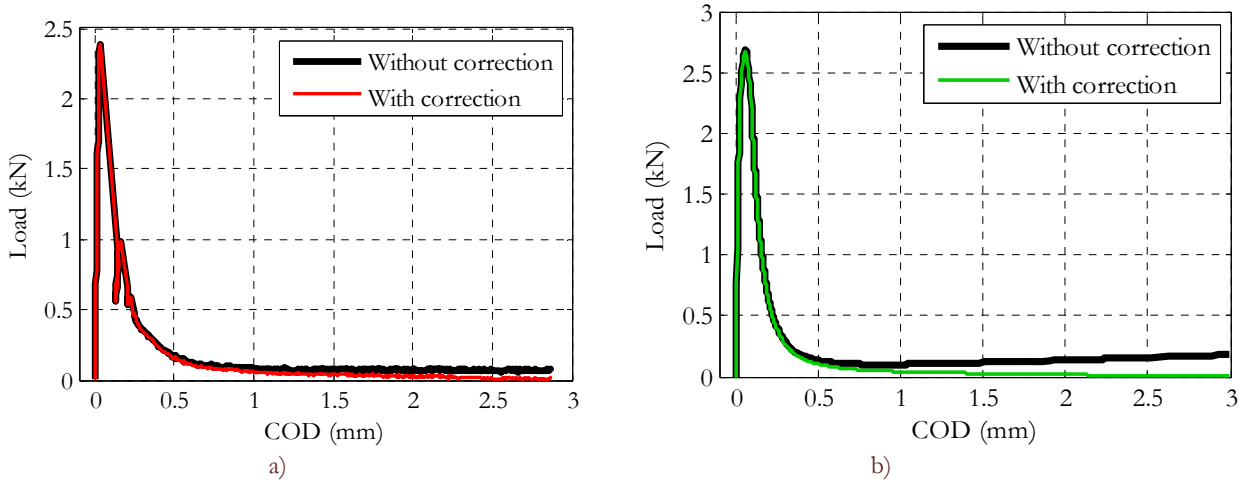

Figure 12: Original and corrected fracture energy curves for specimen 1: a) experimental and b) numerical results.

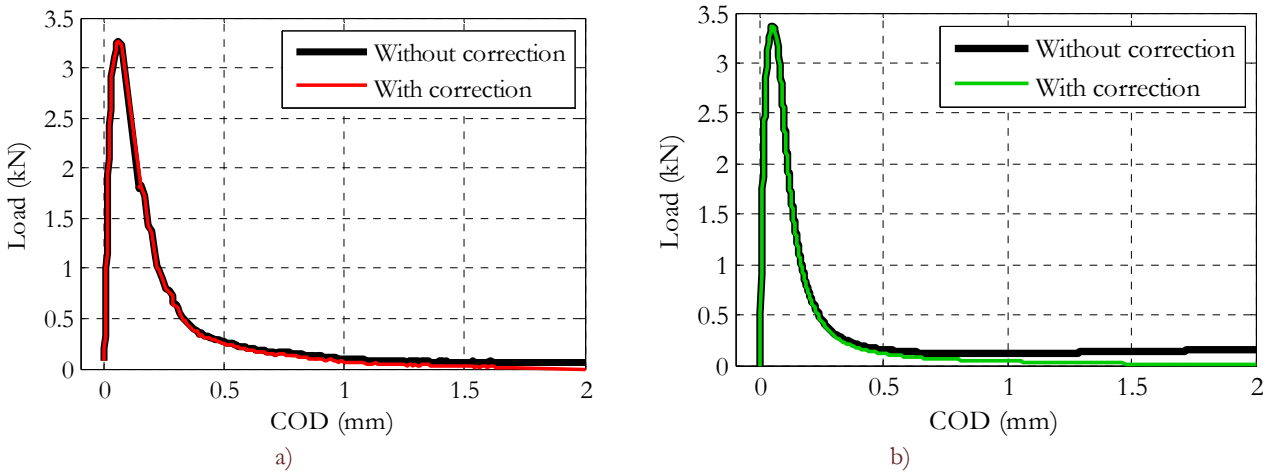

Figure 13: Original and corrected fracture energy curves for specimen 2: a) experimental and b) numerical results.

- *Relationship between experimental test and numerical model results*

The results and estimated errors for the former numerical calculations, referred to work energy and fracture energy, and the tests performed are summarized in Tab. 3.

		W_f [J]	G_f [J/m²]	Error [%]
Specimen 1	Experimental	475.4	98.3	0.96
	Simulation	480	99.2	
Specimen 2	Experimental	710.4	127.3	24.2
	Simulation	538.1	96.4	

Table 3. Summary of the numerical and test results.

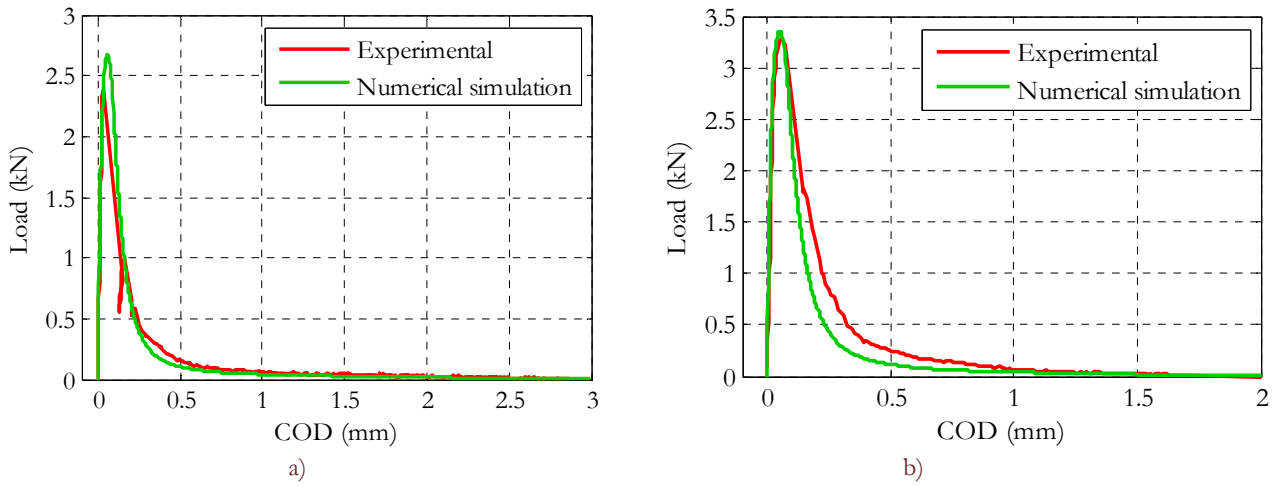

Figure 14: Direct comparison for the experimental and numerical energy curves once corrected. (a) Specimen 1; (b) Specimen 2.

CONCLUSIONS

The principal conclusions derived from this work are the following:

- The 2D simulation implies considering hypothetical bars in which the opening process during testing is achieved by means of prescribing a progressive horizontal displacement of the pulling bars. As a matter of fact, the calculations do not facilitate a reliable reproduction of the real pulling bars bending during testing.
- As a consequence of the inadequate boundary conditions imposed, two effects not occurring during execution of the real test are introduced: a) a parallel opening of the notch lips is enforced so that the factual bending of the pulling bars during testing is not adequately modeled, and b) the transversal free movement of the specimen, necessary for maintaining the geometrical compatibility notch-bar under equilibrium conditions during testing is impeded.
- Both effects implying stiffer solutions lead to an overestimation of the fracture energy in the test simulation compared to the experimental results the first effect having greater influence on the result of the fracture energy.
- Accordingly, 3D calculations are unavoidable to an adequate numerical simulation of the real testing conditions is intended aiming at to facilitate a true value of the fracture energy of the concrete.
- A reasonable agreement between the experimental results and the numerical simulation of the fracture curve is achieved.
- A conversion between the modified compact tension test (MCT) and the standard procedures, i.e. wedge-splitting (WST) and three point (3PB) or four point bending test (4PB) can be now envisaged and justified numerically.

ACKNOWLEDGEMENTS

The investigation reported in this paper was supported by grants M100411204, CZ. 107/2.3.00/20.0214 and FAST-S-14-2532 and projects BIA2010-19920 of the Spanish Ministry of Science and Innovation MICINN and SV-PA-11-012 of the Dept. of Education and Sciences of the Asturias Regional Government.

REFERENCES

[1] Karihaloo, B.L., Fracture Mechanics & Structural Concrete, Longman Scientific & Technical, New York (1995).
[2] Cifuentes, H., Alcalde, M., Medina, F., Comparison of the size-independent fracture energy of concrete obtained by two test methods. VIII International Conference on Fracture Mechanics of Concrete and Concrete Structures. FraMCoS-8. Toledo (2013) 1–6.
[3] Cifuentes, H., Alcalde, M., Medina, F., Measuring the Size-Independent Fracture Energy of Concrete. STRAIN: An International Journal For Experimental Mechanics. 49(1) (2013) 54–59.

[4] RILEM Report 5 Fracture Mechanics Test Methods for Concrete (S. P. Shah & A. Carpinteri eds.), Chapman and Hall, London (1991).
[5] RILEM TC-50 FMC Recommendation Determination of the fracture energy of mortar and concrete by means of three-point bend test on notched beams, Materials & Structures (1985).
[6] Brühwiler, E., Wittmann, F.H., The wedge splitting test, a new method of performing stable fracture mechanics tests, Engineering Fracture Mechanics, 35 (1990) 117-125.
[7] Korte, S., Boel, V., De Corte, W., De Schutter, G., Static and fatigue fracture mechanics properties of self-compacting concrete using three-point bending tests and wedge-splitting tests, Construction and Buildings Materials, 57 (2014) 1–8.
[8] Korte, S., Boel, V., De Corte, W., De Schutter, G., Vibrated concrete vs. self-compacting concrete: Comparison of fracture mechanics properties, Key Engineering Materials, 601 (2014) 199–202.
[9] Merta, I., Tschegg, E.K., Fracture energy of natural fibre reinforced concrete, Construction and Building Materials, 40 (2013) 991-997.
[10] Merta, I., Tschegg, E.K., Uniaxial Fracture Energy of Waste Tyre Rubber Concrete, VIII International Conference on Fracture Mechanics of Concrete and Concrete Structures, FraMCoS-8, Toledo (2013) 1–5.
[11] ASTM E399-90, Standard test method for plane-strain fracture toughness of metallic materials, Annual Book of ASTM Standards, Vol. 03.01, ASTM International, (2002) 443–473.
[12] ASTM International Standard E399-06 (2006), Standard test method for linear-elastic method of plane-strain fracture toughness KIC of metallic materials, (2006) 1–32.
[13] Wagoner, M.P., Buttlar, W.G., Paulino, G.H., Disk-shaped compact tension test for asphalt concrete fracture, Experimental Mechanics, 45 (2005) 270–277.
[14] Linsbauer, H.N., Tschegg, E.K.., Fracture energy determination of concrete with cube-shaped specimens, Zement und Beton, 31 (1986) 38–40.
[15] Cifuentes, H., Medina F., Fracture mechanics applied to concrete (in Spanish), Servicio de Publicaciones, Universidad de Sevilla, Sevilla, (2013).
[16] Červenka Consulting, http://www.cervenka.cz - ATENA Program Documentation, Theory and User Manual
[17] Cervenka, V., Cervenka, J., Pukl, R., ATENA – A tool for engineering analysis of fracture in concrete, Sadhama-Academy Proceedings in Engineering Sciences, 27(4) (2002) 485–492.
[18] ABAQUS/CAE Documentation. Analysis User's Manual: Materials.
[19] Holušová, T., Seitl, S., Fernández-Canteli, A., Numerical support of experimental compact tension test on concrete cylindric specimens, Transactions of the VŠB – Technical University of Ostrava, Civil Engineering Series, No. 1 Vol. XIV, (2014).
[20] Holušová, T., Seitl, S., Fernández-Canteli, A., Numerical simulation of modified compact tension test depicting of experimental measurement by ARAMIS, Key Engineering Materials (2015).
[21] Holušová, T., Seitl, S., Fernández-Canteli, A., Comparison of fracture energy values obtained from 3PB, WST and CT test configurations, Advanced Material Research Journal, 969 (2014) 89–92.
[22] Hillerborg, A., Modeer, M., Petersson, P.E. Analysis of crack formation and crack growth in concrete by means of fracture mechanics and finite elements, Cem Concr Res, 6 (1976) 773–782.